

Fig. 4. Typical conversion cycle for a double slope ADC with DDS.

is dominated by quantization in the ADC. However, at high light levels, the pixel output is limited by illumination shot noise such that 8b resolution is usually sufficient. Furthermore, typical image processing applications such as application of gamma correction expand low pixel values and compress high pixel values. Therefore to take advantage of these characteristics, a double slope ADC was implemented which provides high resolution at low pixel values with a shallow slope analog ramp and later switches to high dynamic range at high pixel values with a steep slope analog ramp. Since the analog ramp and digital counter are both synchronized and have programmable step sizes, the converter resolution is enhanced for low pixel values which require fine digital codes. Similarly, the converter dynamic range is enhanced for high pixel values which use coarser digital codes since they are dominated by illumination shot noise by using a programmable double slope ramp generator. Finally, the DDS operation is quite important and provides a type of random 10b dither to prevent quantization artifacts when in the expanded dynamic range of the converter.

Fig 4 illustrates a typical conversion cycle for double slope ADC with DDS. At (1) pixel reset gate switched off, and resulting output node voltage is converted and stored as reference level (2-4). Photocharge is transferred to sensing node by toggling pixel transfer gate (5-6), and the resulting voltage level is again converted (7-10). However, the double slope technique switches to a steeper slope analog ramp voltage and associated larger counter increment to realize a wider dynamic range within the same number of clock cycles. Change in output voltage is directly proportional to photocharge and is computed by digitally subtracting the two converted data. As seen in Fig 4, the dynamic range is enhanced compared to a simple single slope ADC plotted in dashed line. Using a programmable analog ramp and digital counter increment size, the implemented double slope ADC bank was designed for 10b resolution for the low inputs, 8b SNR for the high level inputs and an overall 10b dynamic range.

## 5. MEASUREMENTS AND RESULTS

Accurate measurements of  $8 \times 8 \mu\text{m}^2$  blocks of the rectangular PD pixel and square PD pixel were taken under the same illumination conditions. The results are summarized to Table 1.

The fill factor simply represents the actual area of the PD

Table 1. Summary of Pixel Characteristics

Pixel Type	Rec. PD	Squ. PD
Pixel Size	$8 \times 8 \mu\text{m}^2$	$8 \times 8 \mu\text{m}^2$
Fill Factor	28.13 %	26.25 %
Effective Fill Factor	75 %	90 %
Min. Illumination	0.7 lux	0.35 lux
Dynamic Range	25 dB	36 dB
Sensitivity	3.65V/lux-sec	3.8V/lux-sec
$G_R G_B$ crosstalk.	10 %	0 %
Pixel Uniformity	5.9 @ 150	2.3 @ 150
Dark Current	$\sim 25 \text{ pA/cm}^2$	$\sim 25 \text{ pA/cm}^2$

without consideration of any microlens structure. The effective fill factor is estimated from the size and shape and efficiency of the microlens. Minimum illumination is defined as the illumination required for minimum measurable pixel output at 30msec exposure with f2.0 lens aperature. Dynamic range is measured as the ratio of the maximum illumination that can be measured without saturating the pixel and minimum illumination with 30msec exposure. Sensitivity is measured as the resulting green pixel output under uniform white illumination at 4700 K.  $G_R G_B$  crosstalk is measured as the difference between green pixels from green-red and green-blue rows under uniform white illumination at 4700 K and is closely related to imager MTF. Pixel uniformity is measured as the standard deviation of pixel outputs when the average has a code count of 150 and under uniform white illumination at 4700 K and with proper gain adjustments on red, green and blue channels. Dark current was measured in the dark at room temperature with integration times ranging from 500msec to 2 sec.

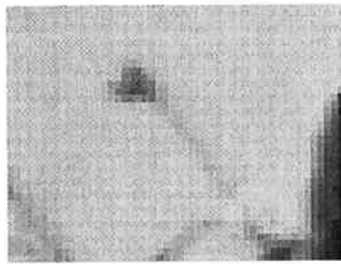
The optimized square PD pixel demonstrated significantly lower  $G_R G_B$  crosstalk as shown in Fig 5. These noise reductions also improve image compression efficiency and dynamic range. Although the square PD pixel had a slightly smaller PD, the higher efficiency microlens contributed to higher sensitivity compared to the rectangular PD pixel. Similarly, the square PD pixel showed better pixel matching as shown in Fig 6. DDS provides excellent cancellation of fixed pattern noise, and remaining pixel mismatches are primarily random.

The double slope ADC is currently still under testing. Preliminary results demonstrate that the ADC circuitry is fully functional and provides enhanced resolution and dynamic range.

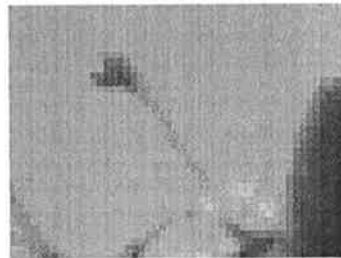
## 6. CONCLUSIONS

A  $640 \times 480$  VGA CMOS imager with a new optically improved pixel layout and 10b ADC bank using a double slope technique was designed and implemented in a modified  $0.5 \mu\text{m}$  DRAM process. Photodiode shape and surface topology were considered in the pixel design and yielded significant improvement in the pixel optical performance.

A die photograph of the implemented chip is shown in Fig. 7

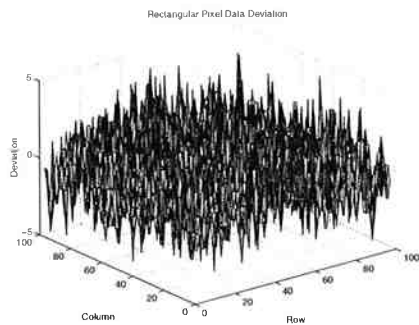


(a) The rectangular PD Pixel Image, mosaic noise,

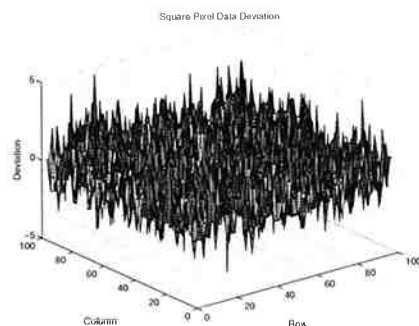


(b) The square PD pixel Image

Fig. 5. Color mosaic noise due to the sensitivity difference between two green types.



(a) Deviations of 100 X 100 Rectangular PD Pixels



(b) Deviations of 100 X 100 Square PD pixels

Fig. 6. Deviations of pixels in a same frame.

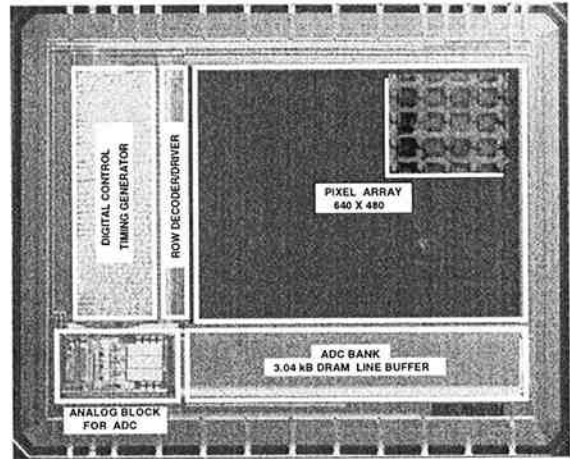


Fig. 7. Die photo of 640x480 CMOS imager.

## 7. ACKNOWLEDGEMENTS

The authors wish to thank Seong-Cheol Byun, Young-Min Lee and Seong-Bin Park in the Device Engineering Laboratory and Process Technology Laboratory of Hyundai Electronics for their support of this project. In addition, we wish to thank Duk-Won Lee for helping to prepare this paper and for his helpful comments.

## REFERENCES

- [1] Woodward Yang, Oh-Bong Kwon, Ju-Il Lee, Gyu-Tae Hwang, and Suk-Joong Lee, " An Integrated 800 X 600 CMOS Imaging System , " in *ISSCC Dig. Tech. Papers* , 1999, pp. 304-305.
- [2] Sunetra. K. Mendis, S. E. Kemeny, R. C. Gee, and Bedabrata Pain, C. O. Staller, Quiesup Kim, Eric R. Fossum, " CMOS Active Pixel Image Sensors for Highly Integrated Imaging Systems , " *IEEE J. Solid-State Circuits* , vol. 32, no. 2, pp. 187-197, Feb., 1997
- [3] Orly Yadid-Pecht, Bedabrata Pain, Craig Staller, Christopher Clark, and Eric R. Fossum, " CMOS Active Pixel Sensor Star Tracker with Regional Electronic Shutter , " *IEEE J. Solid-State Circuits* , vol. 32, no. 2, pp. 285-288, Feb., 1997
- [4] D. J. Friedman and W. Yang, " An Interline CCD Imaging Array with On-Chip A/D Conversion , " in *Proc of SPIE, Charge-Coupled Devices and Solid State Optical Sensors IV* , vol 2172, pp. 54-63, (Bellingham, Washington, 1994)
- [5] Steven Decker, R. Daniel McGrath, Kevin Brehmer, and Charles G. Sodini, " A 256 × 256 CMOS Imaging Array with Wide Dynamic Range Pixels and Column-Parallel Digital Output , " *IEEE J. Solid-State Circuits* , vol. 33, no. 12, pp. 2081-2091, Dec., 1998
- [6] Hon-Sum Wong, " Technology and Device Scaling Considerations for CMOS Imagers , " *IEEE Trans. Electron Devices* , vol. 43, no. 12, pp. 2131-2142, Dec., 1996